Regulated Photon Transport in Chaotic Microcavities by Tailoring Phase Space

Yan-Jun Qian,[1] Hui Liu,[1] Qi-Tao Cao,[1] Julius Kullig,[2] Kexiu Rong,[1] Cheng-Wei Qiu,[3] Jan Wiersig,[2] Qihuang Gong,[1,4] Jianjun Chen,[5,*] and Yun-Feng Xiao[1,4,†]

[1]*State Key Laboratory for Mesoscopic Physics and Frontiers Science Center for Nano-optoelectronics, School of Physics, Peking University, 100871 Beijing, China*

[2]*Institute for Physics, Otto von Guericke University Magdeburg, D-39016 Magdeburg, Germany*

[3]*Department of Electrical and Computer Engineering, National University of Singapore, 4 Engineering Drive 3, Singapore 117583, Singapore*

[4]*Collaborative Innovation Center of Extreme Optics, Shanxi University, Taiyuan 030006, China*

[5]*Department of Physics and Applied Optics Beijing Area Major Laboratory, Beijing Normal University, Beijing 100875, China*

(Received 2 September 2021; accepted 2 December 2021; published 28 December 2021)

Manipulating light dynamics in optical microcavities has been made mainly either in real or momentum space. Here we report a phase-space tailoring scheme, simultaneously incorporating spatial and momentum dimensions, to enable deterministic and *in situ* regulation of photon transport in a chaotic microcavity. In the time domain, the chaotic photon transport to the leaky region can be suppressed, and the cavity resonant modes show stronger temporal confinement with quality factors being improved by more than 1 order of magnitude. In the spatial domain, the emission direction of the cavity field is controlled on demand through rerouting chaotic photons to a desired channel, which is verified experimentally by the far-field pattern of a quantum-dot microlaser. This work paves a way to *in situ* study of chaotic physics and promoting advanced applications such as arbitrary light routing, ultrafast random bit generation, and multifunctional on-chip lasers.

DOI: 10.1103/PhysRevLett.127.273902

Optical microcavities lay the cornerstone in diverse fields, such as quantum optics, coherent light sources, and photonic circuits [1–5]. Over the past decades, much effort has been devoted to manipulating optical fields in microcavities, enabling fundamental physics studies, and superior functional devices. Typically, previous research was classified by two operation domains: (i) in *real space*, mode-field distribution is engineered by designing the cavity structure or incorporating surface plasmon, providing capabilities for field-enhanced applications such as nanolasers [6,7], ultrasensitive sensing [8–11], and quantum information processing [12,13]; (ii) in *momentum space*, by engineering the mode dispersion or controlling the propagation direction, advanced photonic devices are realized, including soliton microcombs [3,14], single-photon routing [15,16], and exceptional-point sensors [17–19].

Besides, *phase space*, spanned by generalized coordinates and their conjugate momenta, provides a comprehensive description of a dynamical system and thus is crucial in modern physics, involving quantum mechanics, condensed-matter physics, thermodynamics, and statistical mechanics [20,21]. The rich structure of the phase space of an asymmetric microcavity was first studied by Nöckel *et al.* [22,23]. Recently, dynamical processes in phase space have promoted numerous applications, such as free-space routing [24–26], level statistics [27,28], and broadband momentum transformation [29,30]. Generally, these studies rely on the design of cavity boundary shape, and the phase space is changed only holistically, instead of a position-specific control of a particular dynamical orbit. Such a limit severely rules out access to the on-demand manipulation of light dynamics in phase space, hindering the further applications with asymmetric microcavities and *in situ* studies on wave chaos, such as chaotic transport [31–33], dynamical localization [34–36], and tunneling [37–40]. Although an alternative scheme by inserting a circular-shaped inclusion into a microdisk, i.e., annular cavity is proposed theoretically to modify phase space [41–44], a local control of specific orbits in phase space is still unrealized and remains challenging. In this Letter, we propose to tailor the phase space to precisely regulate photon transport dynamics in a chaotic microcavity. Through inserting defect perturbations inside an asymmetric microcavity to intercept the leaky path in phase space, a great increase of quality (Q) factor is obtained by more than 1 order of magnitude, showing highly confined optical resonances in the time domain. Moreover, the spatial emission directions of light can be manipulated on demand by reconstructing the output transport channel. This phenomenon is verified experimentally through monitoring the far-field pattern (FFP) of a quantum-dot microlaser.

As shown in Fig. 1(a), the trajectories of light rays in a microcavity can be projected into the reduced phase space (Poincaré surface of section), which is spanned by Birkhoff

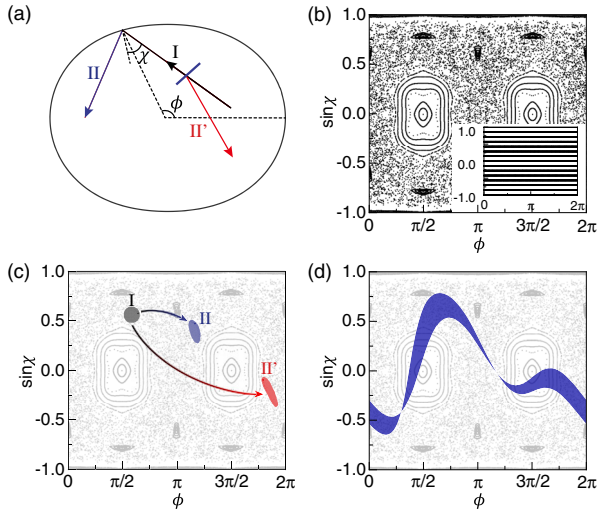

FIG. 1. (a) Ray trajectories in an asymmetric microcavity. Blue segment: a reflective line-defect tailor. I: incident light, II nd II′: light ray without and with the tailor. (b) Ray dynamics in the phase space of the microcavity in (a), where the inset is for a circular cavity. (c) Projection of the light beams I, II, and II′ into phase space, where the incident beam is initialized with a Gaussian transverse profile. (d) Tailored area in phase space by the line-defect tailor in (a).

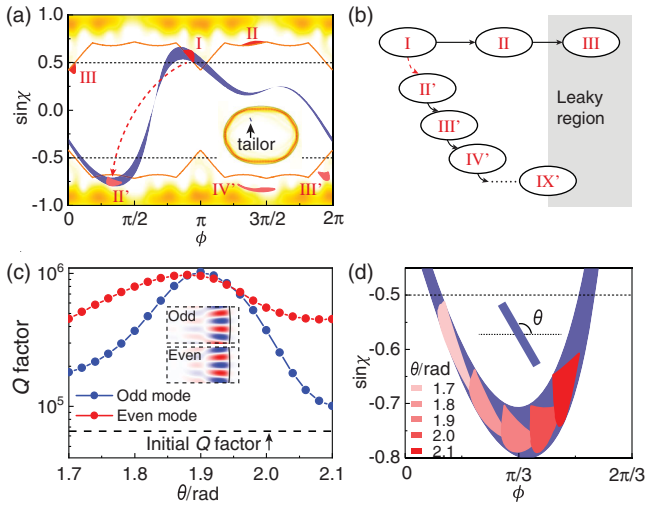

FIG. 2. (a) Manipulation of the photon temporal confinement. Yellow plot: field distribution in phase space of a WGM. Orange curves: partial barriers for confining the WGM. Blue ribbon: tailored region with a line defect shown in the inset. Black dashed lines: critical lines of total internal reflection. Flux sequence I → II → III displays the leaky path without the tailor. II', III' and IV': the first three iterations of flux I with a line-defect tailor. Inset: distribution of the WGM in real space. (b) Schematic of the leaky path in (a). (c) Q factors of odd and even WGMs versus orientation angle θ of the reflective tailor. Insets: Enlarged spatial field distributions. (d) Dependence of flux II' on θ. Tailor parameters: center coordinate $(\pm 0.3R_0,\ \pm 0.479R_0)$, length $\sim 0.12R_0$, line thickness $\sim 0.015R_0$, refractive index $\sim 0.5 + 10\mathrm{i}$.

coordinates [22,45], i.e., the azimuthal angle ϕ and the incident angle χ. In a circular microcavity, the angular momentum of intracavity light is conserved, leading to invariant lines in phase space [inset of Fig. 1(b)]. When the cavity boundary is deformed, various orbit structures emerge in phase space, including Kolmogorov-Arnol'd-Moser (KAM) curves, short-period orbits, and chaotic sea [Fig. 1(b)] [31,46]. In particular, the chaotic sea can serve as a rapid channel for photon transport which is pivotal in momentum transformation, quantum localization, unidirectional emission, etc. [29,31]. Here, the boundary of the deformed cavity is a typical quadrupolar shape defined as $R(\phi) = R_0[1 + \varepsilon\cos(2\phi)]$ [31,46,47], where R_0 decides the cavity size and ε is the deformation parameter ($\varepsilon = 0.12$ if not indicated otherwise).

By inserting a line defect into the deformed cavity, the photon transport dynamics is regulated, where the incident beam can be either absorbed or reflected into another path, depending on the permittivity of the tailor, as shown in Figs. 1(a) and 1(c). Graphically, the phase space is tailored by the defect, exhibiting a ribbonlike region [Fig. 1(d)] which can be tuned by multiple degrees of freedom such as the central position, orientation, and geometry of this defect. When different structures in the phase space such as KAM curves or short-period orbits are hit by the tailor, the corresponding trajectories are interrupted, resulting in selective suppression of high-Q whispering-gallery modes (WGMs) or island modes by several orders of magnitude as desired. Dramatically, this phase-space tailor can be utilized to manipulate chaotic dynamics, and in the following we will show two examples for controlling the temporal confinement and spatial emission of cavity modes by regulating the chaotic photon transport.

In the chaotic cavity, photons can be confined by a characteristic structure named *partial barrier* [orange curves in Fig. 2(a)], which divides the phase space into two nearly isolated subregions [32,35,48,49]. Resonant modes are formed in one of the subregions [yellow plot in Fig. 2(a)], where the mode can transport across the barrier only at turnstile structures in phase space [50], such as fluxes I, II, III in Fig. 2(a). Eventually, after the turnstile transport I → II → III, the photons at flux III enter the leaky region with the incident angle smaller than the critical angle of total internal reflection [Fig. 2(b)], contributing to the loss of the resonant modes. When a line-defect tailor with high reflectivity is introduced into the cavity, we show that the phase space is tailored by a ribbonlike area, and the aforementioned leakage can be intercepted as desired. It is found that the flux I through the turnstile can be *in situ* redirected to a new flux II′ in the opposite propagating direction by deliberately designing the tailored area. In the following motions, the photon flux keeps itself inside the cavity experiencing total reflections for much more times (II′ → III′ → IV′ → … → IX′), until partially touching the leaky region [51]. Thus, with the rising lifetime of the

intracavity photon, the resonant modes will experience lower loss, and the Q factors are expected to increase significantly.

The wave simulation is then conducted to demonstrate this improvement of temporal confinement by tailoring the phase space of a two-dimensional asymmetric microcavity. By employing the finite-element method for the simulation at the 1550 nm band, a pair of nearly degenerate transverse-electric eigenmodes are observed with different parity, i.e., the odd and even WGMs [53], of which their initial Q factors are calculated to be about 6.51×10^4 [Fig. 2(c)]. Considering the mirror symmetry of the quadrupolar cavity, four gold tailors with high reflectivity are symmetrically assigned to intercept all four leaky paths of the WGMs, and the dependence of the improved Q factors on the orientation angle θ of the tailors is plotted in Fig. 2(c). Especially, the highest Q factors are obtained as 1.03×10^6 (9.74×10^5) for the odd (even) mode at $\theta/\mathrm{rad} \sim 1.9$, showing an improvement exceeding 1 order of magnitude compared with the case without tailors. This is because the flux II' travels inside the tailored area when varying the orientation angle of the defect, and reaches the maximum of angular momentum at $\theta/\mathrm{rad} \sim 1.9$, as shown in Fig. 2(d). It is also noticed that the difference of Q factors between odd and even modes may come from the external coupling in wave regimes [54].

Besides the temporal confinement of the photons, the spatial emission direction of the cavity field can also be engineered by constructing the chaotic photon transport channel with the phase-space tailor. Generally, the microcavity emission pattern is obtained by analyzing the chaotic transport dynamics in phase space, where the leaky fluxes III in both Figs. 2(a) and 3(a) result in the directional output emission [51]. By introducing a defect tailor into the cavity, the antecedent flux before the leakage can be tailored, so that the spatial emission is on-demand controlled by engineering the subsequent chaotic transport. When the defect is set as a perfect absorber covering flux I, the photon transport I → II is terminated. Hence, the refractive emission from the subsequent flux III under the critical line [dashed line in Fig. 3(a)] is forbidden, resulting in the elimination of the corresponding emission peak 3, while the rest of far-field emission peaks from other transport paths are preserved well as seen in the upper panel of Fig. 3(b). Correspondingly, the dynamic output in phase space is shown in Fig. 3(c) by the ray-model simulation, where the whole phase space is initialized with uniform energy intensity distribution [51] and the eliminated emission is marked by the dashed circle. It is noted that the other emission peaks can be also removed and only one is retained by inserting the corresponding tailors, leading to the unidirectional far-field emission. When the defect is set as a perfect reflector, a new transport path is constructed, where the flux I is redirected to II′ as presented in Fig. 3(a). Thus, the original emission peak 3 at 1.35π is transferred to peak 3′ at 0.81π in the far field as shown in Fig. 3(b), of which the near-field output is revealed in phase space [Fig. 3(c)]. Note that the transport can also be modulated at other fluxes, such as II or III, for multiple manipulations of far-field emission, which sustains the compatibility of this strategy for different cavity boundaries and refractive index.

In the experiment, we demonstrate the tailor-engineered photon transport by applying a colloidal-quantum-dot (CQD) microlaser using a quadrupolar cavity with $R_0 = 10\ \mu$m, as shown in Fig. 4(a). The asymmetric microcavity is fabricated by exposing a polymer film using electron beam lithography and then filling it with CQD solution after etching the exposed part, while the tailor is formed by unexposing a particular region inside the cavity [51]. Under the pump with a pulse width of 200 ps at 532 nm, the multimode lasing signals are generated at

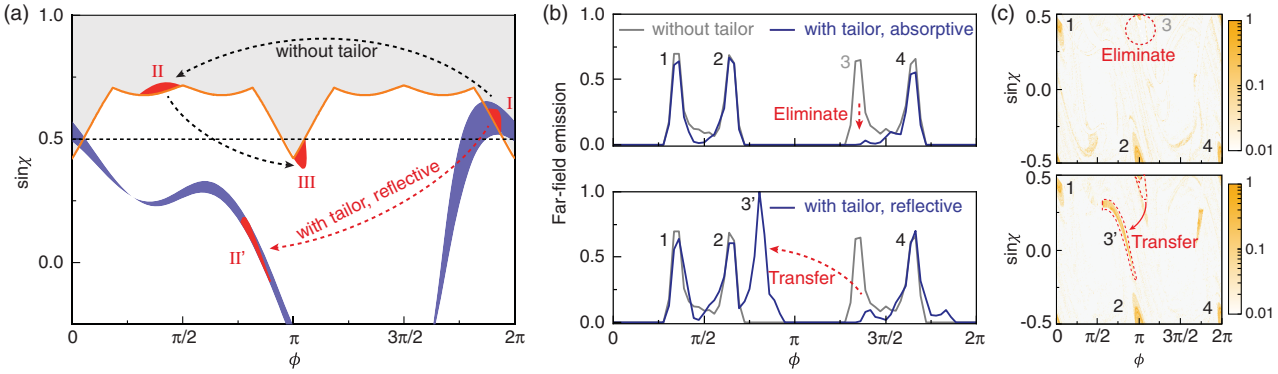

FIG. 3. (a) Photon transport in the chaotic region without or with a tailor. Gray shadow: the localization region by the partial barrier presented as the orange curve. Blue ribbon: tailored region in phase space. I, II, and III are three typical fluxes in the transport process without the tailor. II' is the transferred flux from I by the reflective tailor. (b) Far-field emission of the asymmetric microcavity without a tailor or with an absorptive/reflective tailor. (c) Accumulated energy output under the critical line for the cavity with an absorptive or reflective tailor. The spots marked in sequence correspond to the emission peaks in (b). Tailor parameters: center coordinate $(0.39R_0, -0.46R_0)$, length $\sim 0.12R_0$, orientation $\theta/\mathrm{rad} \sim 1.36$.

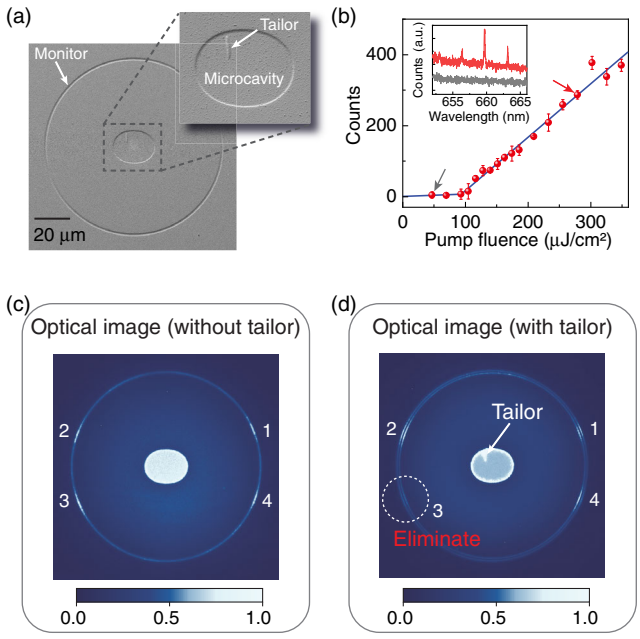

FIG. 4. (a) Scanning-electric-microscope image of the asymmetric microcavity, where the radius parameter $R_0 = 10$ μm and the thickness of the cavity is about 300 nm. (b) Dependence of lasing emission intensities on pump fluences with a tailor. Inset: optical spectra below and above the lasing threshold as marked by the arrows. (c) and (d) Measured FFPs of the laser without and with a tailor, where the emission spots on the surrounding ring are marked as 1–4.

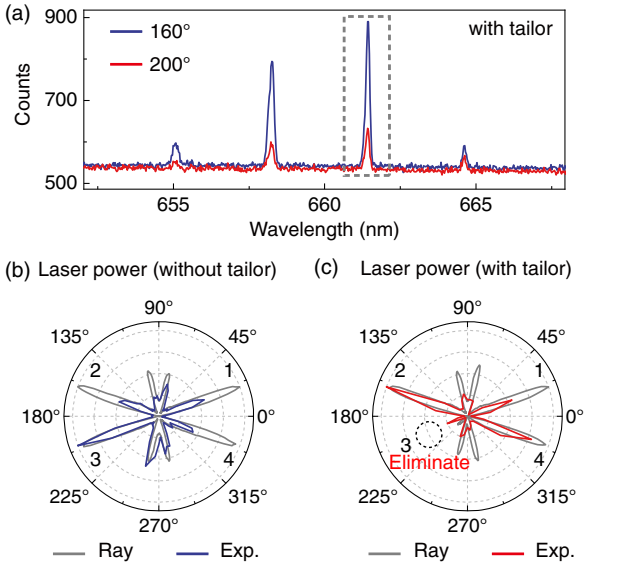

FIG. 5. (a) Lasing spectra at azimuthal angles of 160° and 200°, where the strongest emission peaks are marked by the dashed rectangle. (b) and (c) Experimental far-field emission of the strongest lasing mode for the cavity without and with a tailor. The gray curves present the far-field emission pattern by the ray model.

660 nm band as presented in the inset of Fig. 4(b). The strongest emission intensity depending on the pump fluences is depicted in Fig. 4(b), showing the lasing threshold of 93.37 $\mu J/cm^2$.

Surrounding the microcavity, a ring with a radius of $5R_0$ and a width of 1 μm is etched to serve as a monitor to display the FFP of the microlaser by out-plane scattering. Afterward, the FFP is directly observed by a camera while the microcavity is in the lasing regime (see measurement setup in [51]). For a cavity without the tailor [Fig. 4(c)], four bright spots emerge on the surrounding ring monitor, agreeing well with the expected quadrupolar-emission characteristic. For a cavity with the tailor [Fig. 4(d)] that can be treated as an absorber because of the out-plane scattering, the light spot 3 is eliminated at the ring monitor as shown by the dashed circle, which is consistent with the theoretical prediction [51]. Furthermore, the FFP is characterized by the lasing spectra of one mode in multimode lasers, which is demonstrated by selectively collecting the light at different azimuthal angles of the surrounding ring through a movable pinhole [51]. By recording the intensity of the strongest lasing mode, as denoted by the dashed rectangle in Fig. 5(a), the FFPs of the microlaser without and with the tailor, are plotted in Figs. 5(b) and 5(c), respectively. It is found that the far-field emission 3 at 200° is eliminated by tailoring the phase space, agreeing well with the theoretical design and the optical image captured by the camera. The measured extinction ratio of the emission at 200° is over 3.5 compared with that at 160°, and it can be further boosted by increasing the dissipation of the tailor. Notably, benefiting from excluding the fluorescence background, the fine structures, i.e., two pairs of subpeaks around 90° and 270°, are clearly observed in the far-field by the laser spectra of the mode at ~662 nm, which derives from the low refractive index of the quadrupolar cavity [51].

In summary, we have demonstrated the *in situ* regulation of photon transport in a chaotic microcavity by tailoring its phase space. The temporal confinement is enhanced by redirecting the leaky transport channel to a long-lived path, so that the Q factor of the resonant mode is increased over 1 order of magnitude. Moreover, the spatial far-field pattern of the cavity mode is engineered through constructing a desired emission channel, which is verified experimentally by a quantum-dot microlaser. Note that although intracavity defect perturbations have been used previously for manipulating light fields [17,55], these studies aim at the dynamics in either real or momentum space, of which the underlying physics is fundamentally distinct from manipulating photons in phase space by this work. Furthermore, this strategy can be readily extended to many other fundamental studies as phase space is ubiquitous in nature. For example, the control of system openness by tailoring phase space can promote a comprehensive study of non-Hermitian physics, and the engineering of the temporal confinement may stimulate the exploration of

tunneling dynamics [44,45,56]. The *in situ* perturbation method makes it flexible to control specific structures in phase space, such as constructing an artificial partial barrier and revealing dynamical localization in a chaotic saddle [32,33,48]. Besides, the multidimension manipulation of this work makes it promising for advanced photonic applications, such as ultrafast random bit generation, photonic computing, and multifunctional lasers [30,57,58].

Y.-J. Qian, H. Liu, and Q.-T. Cao contributed equally. We acknowledge helpful discussions with Y.-Z. Gu, L.-K. Chen, W. Liu, A. Gao, Q. Song, and J. Liu. This project is supported by the National Key R&D Program of China (Grants No. 2018YFA0704400, No. 2018YFB2200401), the National Natural Science Foundation of China (Grants No. 11825402, No. 11654003, No. 61922002, No. 91850103, No. 12174010), the Beijing Natural Science Foundation (Grant No. Z180015), Beijing Municipal Science & Technology Commission No. Z201100004020007, and the High-performance Computing Platform of Peking University. Q.-T. Cao is supported by the National Postdoctoral Program for Innovative Talents (Grant No. BX20200014) and the China Postdoctoral Science Foundation (Grant No. 2020M680185).

*jjchern@bnu.edu.cn
†yfxiao@pku.edu.cn

[1] H. J. Kimble, Nature (London) **453**, 1023 (2008).
[2] P. Lodahl, S. Mahmoodian, S. Stobbe, A. Rauschenbeutel, P. Schneeweiss, J. Volz, H. Pichler, and P. Zoller, Nature (London) **541**, 473 (2017).
[3] T. J. Kippenberg, A. L. Gaeta, M. Lipson, and M. L. Gorodetsky, Science **361**, 8083 (2018).
[4] H. Deng, G. L. Lippi, J. Mrk, J. Wiersig, and S. Reitzenstein, Adv. Opt. Mater. **9**, 2100415 (2021).
[5] Q. Xu, B. Schmidt, S. Pradhan, and M. Lipson, Nature (London) **435**, 325 (2005).
[6] M. Noginov, G. Zhu, A. Belgrave, R. Bakker, V. Shalaev, E. Narimanov, S. Stout, E. Herz, T. Suteewong, and U. Wiesner, Nature (London) **460**, 1110 (2009).
[7] R. F. Oulton, V. J. Sorger, T. Zentgraf, R.-M. Ma, C. Gladden, L. Dai, G. Bartal, and X. Zhang, Nature (London) **461**, 629 (2009).
[8] Y.-F. Xiao, C.-L. Zou, B.-B. Li, Y. Li, C.-H. Dong, Z.-F. Han, and Q. Gong, Phys. Rev. Lett. **105**, 153902 (2010).
[9] J. D. Swaim, J. Knittel, and W. P. Bowen, Appl. Phys. Lett. **99**, 243109 (2011).
[10] M. D. Baaske and F. Vollmer, Nat. Photonics **10**, 733 (2016).
[11] J. M. Ward, Y. Yang, F. Lei, X.-C. Yu, Y.-F. Xiao, and S. N. Chormaic, Optica **5**, 674 (2018).
[12] Y. Yin, S. Li, S. Böttner, F. Yuan, S. Giudicatti, E. S. G. Naz, L. Ma, and O. G. Schmidt, Phys. Rev. Lett. **116**, 253904 (2016).
[13] P. Peng, Y.-C. Liu, D. Xu, Q.-T. Cao, G. Lu, Q. Gong, and Y.-F. Xiao, Phys. Rev. Lett. **119**, 233901 (2017).
[14] V. Brasch, M. Geiselmann, T. Herr, G. Lihachev, M. H. Pfeiffer, M. L. Gorodetsky, and T. J. Kippenberg, Science **351**, 357 (2016).
[15] I. Shomroni, S. Rosenblum, Y. Lovsky, O. Bechler, G. Guendelman, and B. Dayan, Science **345**, 903 (2014).
[16] M. Scheucher, A. Hilico, E. Will, J. Volz, and A. Rauschenbeutel, Science **354**, 1577 (2016).
[17] J. Wiersig, Phys. Rev. Lett. **112**, 203901 (2014).
[18] W. Chen, Ş. K. Özdemir, G. Zhao, J. Wiersig, and L. Yang, Nature (London) **548**, 192 (2017).
[19] Y.-H. Lai, Y.-K. Lu, M.-G. Suh, Z. Yuan, and K. Vahala, Nature (London) **576**, 65 (2019).
[20] D. D. Nolte, Phys. Today **63**, No. 4, 33 (2010).
[21] W. P. Schleich, *Quantum Optics in Phase Space* (John Wiley & Sons, New York, 2011).
[22] J. Nöckel, A. Stone, and R. Chang, Opt. Lett. **19**, 1693 (1994).
[23] J. U. Nckel and A. D. Stone, Nature (London) **385**, 45 (1997).
[24] J. Wiersig and M. Hentschel, Phys. Rev. Lett. **100**, 033901 (2008).
[25] Y.-S. Park and H. Wang, Nat. Phys. **5**, 489 (2009).
[26] F. Albert, C. Hopfmann, A. Eberspächer, F. Arnold, M. Emmerling, C. Schneider, S. Höfling, A. Forchel, M. Kamp, J. Wiersig, and R. S, Appl. Phys. Lett. **101**, 021116 (2012).
[27] J. Wiersig and J. Main, Phys. Rev. E **77**, 036205 (2008).
[28] L. Wang, D. Lippolis, Z. Li, X. Jiang, Q. Gong, and Y. Xiao, Phys. Rev. E **93**, 040201(R) (2016).
[29] X. Jiang, L. Shao, S. X. Zhang, X. Yi, J. Wiersig, L. Wang, Q. Gong, M. Lončar, L. Yang, and Y. F. Xiao, Science **358**, 344 (2017).
[30] H.-J. Chen, Q.-X. Ji, H. Wang, Q.-F. Yang, Q.-T. Cao, Q. Gong, X. Yi, and Y.-F. Xiao, Nat. Commun. **11**, 2336 (2020).
[31] H. G. Schwefel, N. B. Rex, H. E. Tureci, R. K. Chang, A. D. Stone, T. Ben-Messaoud, and J. Zyss, J. Opt. Soc. Am. B **21**, 923 (2004).
[32] J.-B. Shim, S.-B. Lee, S. W. Kim, S.-Y. Lee, J. Yang, S. Moon, J.-H. Lee, and K. An, Phys. Rev. Lett. **100**, 174102 (2008).
[33] S. Shinohara, T. Harayama, T. Fukushima, M. Hentschel, T. Sasaki, and E. E. Narimanov, Phys. Rev. Lett. **104**, 163902 (2010).
[34] C. Gmachl, F. Capasso, E. Narimanov, J. U. Nöckel, A. D. Stone, J. Faist, D. L. Sivco, and A. Y. Cho, Science **280**, 1556 (1998).
[35] M. Michler, A. Bäcker, R. Ketzmerick, H.-J. Stöckmann, and S. Tomsovic, Phys. Rev. Lett. **109**, 234101 (2012).
[36] C.-H. Yi, J.-W. Lee, J. Ryu, J.-H. Kim, H.-H. Yu, S. Gwak, K.-R. Oh, J. Wiersig, and C.-M. Kim, Phys. Rev. A **101**, 053809 (2020).
[37] C. Dembowski, H.-D. Gräf, A. Heine, R. Hofferbert, H. Rehfeld, and A. Richter, Phys. Rev. Lett. **84**, 867 (2000).
[38] J. Yang, S.-B. Lee, S. Moon, S.-Y. Lee, S. W. Kim, T. T. A. Dao, J.-H. Lee, and K. An, Phys. Rev. Lett. **104**, 243601 (2010).
[39] S. Gehler, S. Löck, S. Shinohara, A. Bäcker, R. Ketzmerick, U. Kuhl, and H.-J. Stöckmann, Phys. Rev. Lett. **115**, 104101 (2015).

[40] S. Wang, S. Liu, Y. Liu, S. Xiao, Z. Wang, Y. Fan, J. Han, L. Ge, and Q. Song, Light Sci. Appl. **10**, 135 (2021).
[41] M. Cai, O. Painter, and K. J. Vahala, Phys. Rev. Lett. **85**, 74 (2000).
[42] M. Hentschel and K. Richter, Phys. Rev. E **66**, 056207 (2002).
[43] J. Wiersig and M. Hentschel, Phys. Rev. A **73**, 031802(R) (2006).
[44] A. Bäcker, R. Ketzmerick, S. Löck, J. Wiersig, and M. Hentschel, Phys. Rev. A **79**, 063804 (2009).
[45] H. Cao and J. Wiersig, Rev. Mod. Phys. **87**, 61 (2015).
[46] R. Schäfer, U. Kuhl, and H. Stöckmann, New J. Phys. **8**, 46 (2006).
[47] N. B. Rex, H. E. Tureci, H. G. L. Schwefel, R. K. Chang, and A. D. Stone, Phys. Rev. Lett. **88**, 094102 (2002).
[48] J. B. Shim, J. Wiersig, and H. Cao, Phys. Rev. E **84**, 035202 (R) (2011).
[49] Y.-Z. Gu, L.-K. Chen, Y.-J. Qian, Q. Gong, Q.-T. Cao, and Y.-F. Xiao, Phys. Rev. E **102**, 062208 (2020).
[50] J. Meiss, Rev. Mod. Phys. **64**, 795 (1992).
[51] See Supplemental Material at http://link.aps.org/supplemental/10.1103/PhysRevLett.127.273902 for a detailed description of photon evolution in phase space, regulation of chaotic photon transport for leakage manipulation, and experimental measurements, where [52] is included.
[52] K. Rong, F. Gan, K. Shi, S. Chu, and J. Chen, Adv. Mater. **30**, 1706546 (2018).
[53] J. Wiersig, Phys. Rev. A **84**, 063828 (2011).
[54] J. Unterhinninghofen, J. Wiersig, and M. Hentschel, Phys. Rev. E **78**, 016201 (2008).
[55] C. Dembowski, H.-D. Gräf, H. L. Harney, A. Heine, W. D. Heiss, H. Rehfeld, and A. Richter, Phys. Rev. Lett. **86**, 787 (2001).
[56] D. A. Steck, W. H. Oskay, and M. G. Raizen, Science **293**, 274 (2001).
[57] K. Kim, S. Bittner, Y. Zeng, S. Guazzotti, O. Hess, Q. J. Wang, and H. Cao, Science **371**, 948 (2021).
[58] S. Sunada and A. Uchida, Sci. Rep. **9**, 19078 (2019).